Application of Regional Subspace Detection to Identify Mining Related Seismicity

Derrick JA Chambers, Graduate Student
Michael K Mccarter, Professor of Mining Engineering
University of Utah, Department of Mining Engineering
Salt Lake City, UT

Keith D Koper, Professor
Kris L Pankow, Professor
University of Utah, Department of Geology and Geophysics
Salt Lake City, UT

ABSTRACT

In a mining environment, high quality seismic event catalogs are often useful in interpreting local stress states and identifying areas with elevated ground control risk. Installation, operation, and maintenance of local/in-mine seismic networks, however, may be prohibitively expensive, and mine operators may not anticipate the need for seismic data until unusual mining conditions arise. If regional, generally public, seismic instrumentation could be used to reproduce the results generated by local/in-mine instrumentation to an acceptable degree of fidelity, it would be a valuable and inexpensive tool for mine planners and ground control engineers.

In this study we apply subspace detection—a non-traditional seismic event detection technique—to data from a sparse, regional network. The process is employed to identify mining induced seismicity (MIS) from an underground coal district. The results are compared to a seismic event catalog produced by a local seismic array operating within the permit boundaries. Additionally, we analyze the performance of two different stations of the same sparse, regional network in identifying blasts at a surface coal mine for which we have a detailed blasting log. In both cases data from stations between 10 and 60 km away from mining activity are used. We also explore the trade-offs between the number of detections and the number of false positives, which is influenced heavily by detection thresholds and the number of stations used in the process.

For the surface mine we are able to identify more than 90% of the production blasts documented in the blasting log. We also find that the detected blasts from each of the four active pits produce waveforms similar to one another. The results are not dependent on source-receiver distance, and by requiring detections to occur on both stations the number of sure false positives is reduced to zero. In the underground mining district we identify between 30% and 75% of the events detected by the local array, depending on the acceptable number of false positives and the source-receiver distance. We also find many events that were missed by the local array, showing that regional subspace detection can usefully augment traditional local catalogs. Moreover, subspace detection can provide an estimate on event location and classification using data from as little as one seismic station.

INTRODUCTION

The practice of monitoring mining induced seismicity (MIS) can yield valuable information for both mine planning and hazard management. For example, the location and magnitude of seismic events can be a strong indicator of instability (Mendecki, 1997), induced events can be used as a passive source for tomography in which rock properties and stress states can be inferred (Luxbacher et al., 2008), and seismic catalogs can be employed in conjunction with numerical modeling for mine planning purposes (Mercer and Bawden, 2005). Many mines, however, find the installation and maintenance of seismic instrumentation prohibitively expensive, or do not anticipate a need for seismic data until unusual, and potentially dangerous, circumstances arise.

Several mines in the United States are located near regional seismic arrays. One such array (although not a permanent network), the EarthScope Transportable Array (TA) has provided regional seismic monitoring for nearly every mine in the continental United States for a period of about 18 months sometime between 2007 and 2015. Data from TA stations are processed to create the array network facilities (ANF) seismic event catalog. Because station spacings for the TA are approximately 70 km, generally only relatively large-magnitude mining induced events are detected, which limits the usability of the regional seismic data for analysis of small magnitude MIS. Recently, however, waveform similarity detection methods, principally waveform correlation and subspace detection, have been used on regional seismic network data to augment detection capabilities significantly (Gibbons and Ringdal, 2006; Harris, 2006). By applying these methods, low magnitude seismic events can be found that would otherwise be too small to identify. In the case of the Crandall Canyon Mine collapse, cross-correlation techniques were used to identify and locate thousands more collapse-related events than originally cataloged by conventional means. The newly detected events shed light on the collapse sequence and important geological structures (Kubacki et al., 2014).

This study assesses the ability of subspace detection methods to identify mining related seismicity on publically available TA data from 2008 in two distinct mining environments (Figure 1). The

first study area is a surface coal mine located in Wyoming. The surface mine operated four open pits during 2008 and conducted frequent blasting at each of the pits. The mine provided a blasting log, allowing the performance of the subspace detectors to be quantitatively assessed. The second study area is an underground coal mining district in Colorado that employs longwall mining. A local seismic array, known as the North Fork (NF) array, operated and maintained by the Office of Mine Safety and Health Research (OMSHR), monitored the district in 2008 (Swanson et al., 2008). The catalog created by the NF seismic network allows for regional subspace detection performance to be compared with the detection capabilities of the local array using traditional power detectors.

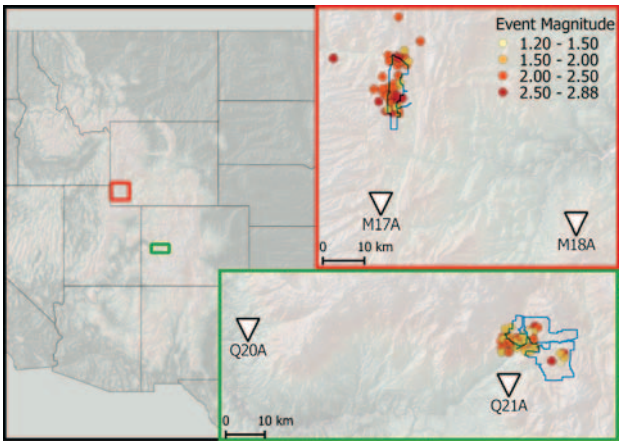

Figure 1. Mining district locations (red and green borders), TA stations used in this study (white inverted triangles) mine permit boundaries (blue polygons), and seismic events in the ANF catalog (dots colored according to local magnitude).

THEORY

A few concepts merit review for those not familiar with waveform similarity detection methods. Although not exhaustive or mathematically rigorous, the following brief introduction should be sufficient to understand the underlying principles of subspace detection.

Seismic Waveforms

The waveforms that are observed on a seismogram are a measure of ground motion (displacement, velocity, or acceleration) as a function of time. The data are usually digitally recorded with a fixed sampling interval (Stein and Wysession, 2009). After removing the filtering effect of the seismic instrument, a given waveform (s) is composed of two elements (Harris, 2006):

$$s(t) = \sum_i \int h_i(\tau) g_i \left(t - \tau, \underline{\xi}, \underline{\chi}\right) d\tau \qquad (1)$$

where h_i is the source time history and g_i is the Green's function for a given source i. The source time history accounts for the physical phenomenon that releases seismic energy (slip on a fault, an explosion, etc.) and its progression through time. The Green's function accounts for the effects of propagation source location to (ξ underscore) the receiver (χ underscore) including scattering, reflection, refraction, etc. If two waveforms are similar, the source time history and Green's function are also similar, implying that the two events occurred in similar locations and were caused by similar sources. Sources that vary only in energy amplitude but that occur in the same location tend to produce similar waveforms that differ only by a scaling factor over some frequency band (Richards et al., 2006 and references therein), which allows the use of waveform matching techniques as an effective detection method (Anstey, 1996).

Cross Correlation

In order to quantify amplitude-independent similarity between two digitized waveforms, vectors X (bar) and Y (bar) of length m and n where m is less than or equal to n, the normalized cross correlation operator can be used, which is defined as:

$$C[i] = \frac{(X[0:m] - \bar{X}[0:m]) * (Y[i:m+i] - \bar{Y}[i:m+i])}{m * \sigma_{X[0:m]} * \sigma_{Y[i:m+i]}} \qquad (2)$$

where brackets indicate indicial ranges and the cross correlation index, i, varies from 0 to $n–m$ +1; sigma indicates the standard deviation; X (bar) and Y (bar)and indicate averages; and the star operator, * , represents multiplication if applied to scalars, or the dot product if applied to vectors. The value of the normalized cross correlation (C) ranges from -1.0 to 1.0. A value of 1.0 indicates that the vectors are identical if one is multiplied by a positive scalar, a value of 0 indicates the vectors are orthogonal, and a value of -1 indicates the vectors are identical if one is multiplied by a negative scalar. In addition to seismic event detection, cross correlation can be used to quantify similarity between a number of known seismic waveforms to form groups, or clusters, based on some similarity requirement (Houser et al., 2008), as well as for more exotic applications such as extracting empirical Green's functions from ambient noise (Bensen et al., 2007).

Singular Value Decomposition

Singular value decomposition (SVD) is a factorization of a matrix, similar to eigenvalue decomposition. Following the notation of Harris (2006), a matrix (X underscore)—the columns of which, in this application, are aligned waveforms—can be written in terms of an orthonormal basis (W underscore), a diagonal matrix of singular values ($\sum$), and a unitary matrix (V underscore):

$$\underline{X} = \underline{W}\underline{\sum}\underline{V}^T \qquad (3)$$

where the superscript T denotes the transpose operation. Often the original matrix (X underscore) can be approximated by:

$$\underline{X} \approx \underline{W}_d \underline{\sum}_d \underline{V}_d^T \qquad (4)$$

where the subscript d denotes truncation: only the d left-most columns of the matrices are retained. The value d, therefore, indicates how many orthonormal vectors are in the basis (W_d underscore) which is formally defined as the dimension of representation.

Vector Projections

A vector (V) of length n can be projected on an n-by-m basis (U):

$$V_p = UU^T V \tag{5}$$

A useful measure of how well the basis U is able to reproduce V, or how well V "fits" into U, is a ratio of the projected vector energy over the original vector energy:

$$C = \frac{V_p^T V_p}{V^T V} \tag{6}$$

where C is referred to by Harris (2006) as the fractional energy capture if U was created using Equation 4 (U - W_d underscore) and V is a column vector of. (X underscore). The fraction of energy captured is one gauge of the validity of Equation 4 for a given X underscore and d. Alternatively, C may be used to test the hypothesis that a signal composed of a linear combination of the column vectors of U is present in V. In the latter case, C is referred to as the detection statistic.

DATA

Seismic Data

The Array Network Facilities (ANF) catalog was downloaded (Array Network Facility, 2013) and queried for all seismic events recorded during the years of 2007 to 2009 with epicenters within 10 km of the mines of interest. ANF processing and location procedures used to create the catalog are outlined in Astiz et al. (2014). Three-component broadband continuous data and event waveform data from four TA stations were downloaded for the entire year of 2008 using the Incorporated Research Intuitions for Seismology (IRIS) web service. Data from stations M17A and M18A (about 15 and 60 km away) were used to study the seismicity originating from the surface mine and data from stations Q21A and Q20A were used to study seismic events from the underground coal district (the stations were located approximately 10 and 50 km away) (Figure 1).

Verification Data

A log of all the production shots at the surface mine in 2008 was provided by the company. The log indicates in which of the four pits each shot occurred, the approximate detonation time, and a few other parameters. OMSHR provided the 2008 catalog of seismic events created using data from the local array deployed above the underground coal district. The catalog (North Fork, or NF catalog) is the result of automatic detections and locations performed using an Earthworm system (Johnson et al., 1996). The software was configured to perform well on a mine-wide scale (Swanson et al., 2008) but the NF catalog has not undergone review by analysts. Helicorder images of the continuous data recorded by each station were also provided. Both the seismic catalog and the blasting log were used for verification purposes, thereby enabling the detector performance to be quantitatively evaluated.

PROCESSING

General Data Processing

The data processing was performed using the python programming language, primarily the package Obspy (Megies et al., 2011) and the subspace detection package Detex (currently in development at the University of Utah). For both the continuous seismic data and the event waveforms, the instrument response was removed, the data were detrended, and the traces were filtered between 1 and 10 Hz. A series of data quality checks were carried out on the hour-long continuous data files to delete files with gaps, clipped waveforms, or missing channels.

Subspace Detection

A workflow similar to the one outlined in Harris (2006) was followed in order to construct subspace detectors from the events recorded in the ANF catalog. First, similarity matrices were created by correlating the waveform from each event-station pair with every other waveform recorded on the same station (Figure 2a, Equation 2). The events were then grouped together using a single link hierarchical clustering algorithm, and dendrograms were created to visualize the grouping (Figure 2b). The required correlation coefficient to define the groups was allowed to vary between stations in order to avoid forming an excessive number of small clusters.

Next, the waveforms were aligned and trimmed to a duration of 30 seconds (Figure 2c). SVD was then performed on the aligned waveforms in order to calculate an orthonormal basis (Figure 2d, Equation 3). The minimum number of vectors from the SVD basis required to represent the group of waveforms adequately was estimated by calculating the average percentage of energy captured as a function of dimension of representation (Figure 2e, Equations 5 and 6). The fewest number singular vectors able to capture an average of 90% of the waveform energy was selected as the basis to represent the original signals (Equation 4).

An empirical estimation of seismic noise (i.e., recorded seismic data with no seismic source signal present) was estimated by calculating the detection statistic (Equations 5 and 6) for each subspace-station pair with 100 hours of continuous data at each time step. Only continuous data segments with no obvious, high-amplitude values were used. A beta distribution was then fit to the resulting detection statistic values via the maximum likelihood method. Using the beta distribution, a value of the detection statistic that set the upper tail probability to 10^{-12} was selected as the threshold for declaring successful detections (Figure 2f) for each subspace-station pair. In theory, when the detection statistic is calculated any value above the threshold determined in this way would have a 10^{-12} likelihood of being a false detection due to incoherent random noise.

A sliding window scheme was applied to the continuous data in conjunction with Equations 5 and 6 to calculate the detection statistic of each station-subspace pair for every time step of the continuous data. The absolute times corresponding to any values in the detection statistic vector that exceeded the determined

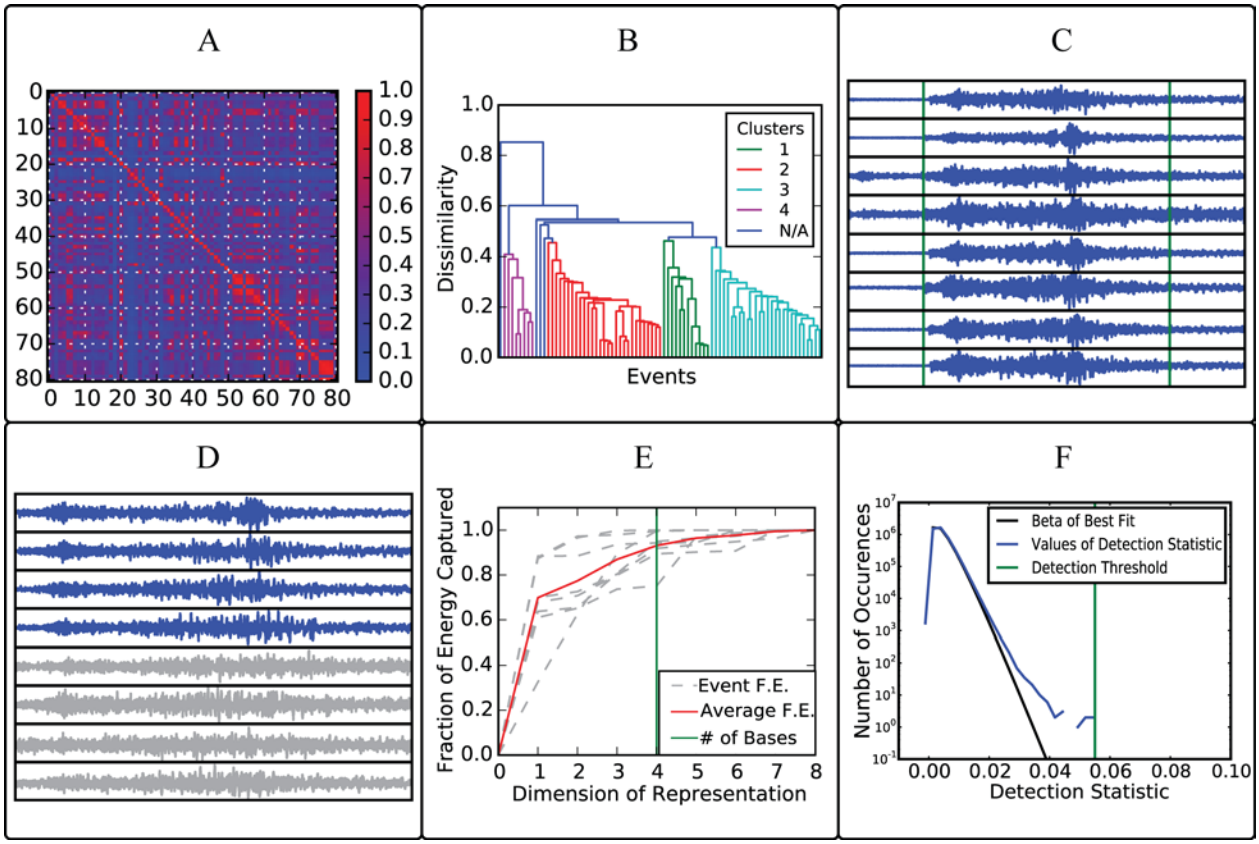

Figure 2. Subspace creation and detection threshold determination using data from M18A. Panel A shows the similarity of each event pair. Diagonal shows autocorrelations. Panel B shows the hierarchical clustering of the waveforms (four clusters, each colored differently). Panel C shows the aligned and trimmed waveforms belonging to the red cluster. Panel D contains the orthonormal basis vectors that are selected (blue) and unused (grey). Panel E shows the criteria for selecting dimension of representation (how many basis vectors to use) requiring the average (red line) of the fractional energy captured of each event (blue dotted lines) to be at least 0.9. Panel E depicts the selection of a detection threshold (green vertical line) based on a beta distribution (black line) fitted to detection statistic values of the subspace and continuous data (blue line).

thresholds were recorded, and magnitudes were estimated with an iterative waveform scaling method similar to that used in Gibbons and Ringdal (2006). Based on the difference between the beginning times for each of the aligned waveforms in the subspace and the corresponding ANF event origin times, a maximum and minimum offset time, essentially a travel time estimate, were made for every subspace. The range defined by the maximum and minimum offset time was used to calculate a range of possible origin times for each detection. Overlaps in the range of predicted origin times were used to associate detections together from different stations.

Detection Verification

For the surface coal mine, it was required that a detection occur within six minutes of the recorded time in the blast log in order to be considered verified. Detections that did not occur within six minutes of an event in the blast log were either classified as "False Detections" (FD) if they occurred at night, or "Unknown" (UK) if they occurred during local business hours. The unknown category was created to account for potential inaccuracies in the log.

The helicorder records of each station in the NF array were parsed in order to find times in which at least 10 of the 16 stations were recording and telemetering data. Only detections occurring during periods where this condition was met were compared against the results in the NF catalog in order to eliminate bias from network downtime.

The number of verified events and non-verified events were both considered in assessing detector performance. The results from individual stations and combinations of stations monitoring the same districts were evaluated.

RESULTS

Surface Mine

Nearly all the blasts were identified on both stations, so only detections occurring on both stations were considered in order to reduce false detections. A total of 345 blasting events were identified out of 376 (~90%) shots recorded in the log. Six detections occurred during local business hours that did not correspond to any potential logged blast (Figure 3a). These were classified as "unknown" (UK). By combining the stations, the number of sure false detections, or events occurring outside business hours, was reduced to zero. When using only a single station, the number of false detections was as high as 300. A

roughly linear relationship exists between the estimated event magnitude and detection statistic (Figure 3b) probably due to lower magnitude events having smaller signal to noise ratios and thus lower detection statistics. Of the 31 shots that were not detected, most were visible by manually inspecting the continuous data of both stations indicating the detectors failure to identify the events was probably not due to the signals having prohibitively low amplitudes.

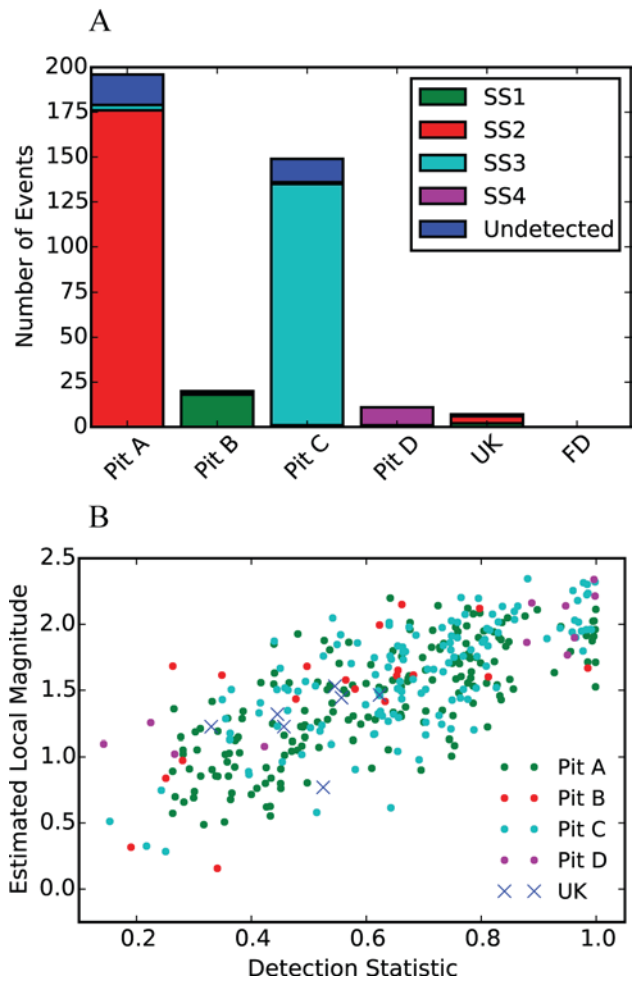

Figure 3. Subspace detector performance for the surface mine. Panel A shows the number of events from each pit detected by each subspace for the combined station results. Events labeled UK are unknown and FD are false detections. Panel B shows the relationship between detection statistic and estimated magnitude.

Underground Mine Results

For station Q21A, 6594 of 9010 (~75%) of the events in the NF catalog were identified with 24930 potential false detections. Using station Q20A, 2916 (~33%) NF events were detected with 7201 false detections. When both stations are used 2823 (~31%) of the NF events are identified with 1361 potential false detections. If the detection threshold were increased, then both the number of detected events and potential false detections would decrease, but not at the same rate (Figure 4a). Some of the potential false detections, particularly from the combined station results, have very high detection statistics. The 18 potential false detections with the highest estimated local magnitude (>1.25) were all identified visually by inspecting the NF helicorder records, indicating that the examined potential false detections were in fact genuine events missed by the NF array.

Assuming equal data quality for Q20A and Q21A, the source-receiver distance plays a large role in the magnitude of events the detectors are able to identify; the closer station (Q21A) was much more effective in finding events with magnitudes 0.5 to 1.25 (Figure 4b) than the further station (Q20A).

The subspaces generally detect events that are closely related spatially (Figure 4c), each subspace corresponding to a different mine within the district. Note that Figure 4 only shows the results for the periods in which 10 NF stations were recording data, and therefore not all detections or ANF events are shown in the figure.

DISCUSSION

The two station detectors at regional distance performed well for finding surface blasts (~90% of events identified), and moderately well for finding MIS produced by the coal mines (~32% of events identified). In both settings, when only a single station is used and the detection thresholds are determined empirically, the number of false positives is unacceptably large. The high number of false detections is often apparent in the misfit of the observed data and fitted theoretical distribution (Figure 2f), which can still occur even when avoiding continuous data with apparent signals. The misfit is generally attributed to rogue transient signals—seismic events not originating from the same source/location as the training events—which share some small degree of similarity with the waveforms used to construct the detector. This explanation is reasonable because events originating in different regions can sometimes be moderately well correlated (Dodge and Walter, 2015). The effects of the undesired signals on the detection results can be mitigated or eliminated by only accepting detections that occur on more than one station (Slinkard et al., 2014). Multi-station detectors produce fewer false detections for two reasons. First, because differential arrival time requirements can be imposed to constrain source location to the area of interest. Second, because adding more complexity to the detector greatly reduces the chance that non-coherent random noise will exceed the threshold. In this study, requiring detections to occur on two stations is successful in greatly reducing the number of false detections. The disadvantage in this case, however, is that the number of potential detections, and the reliably detectable magnitude range, is limited to that of the poorest performing station (Figure 4b).

The surface blasting events listed in the log but missed by the subspace detector were, on average, not lower-amplitude than the detected events, and nearly all the undetected events were visible in the continuous data from the closest station (M17A). One likely explanation of the detector's failure is a significant variance in waveform of the undetected events from the events used to create the detector. Other studies have found that surface blasts occurring in nearly the same location can produce very different waveforms (Bonner et al., 2003; McLaughlin et al., 2004) possibly caused by variation in the free-face orientation, hole delays, explosive agent, or a variety of other blasting practices (Stump et al., 2001).

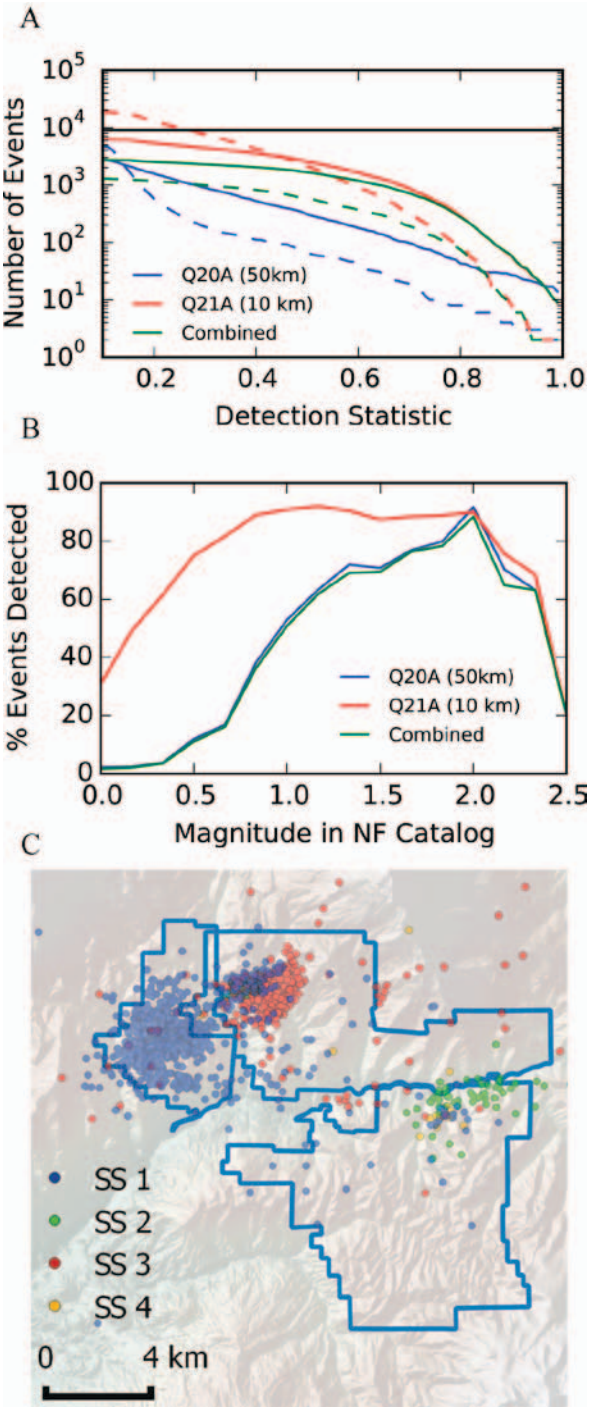

Figure 4. Subspace performance for the underground coal district. Panel A shows the number of verified detections (solid lines), potential false detections (dotted lines), and events in the NF catalog (black solid line) as a function of detection statistic. Panel B shows the percentage of NF events detected by magnitude for each station. Panel C shows the spatial relationship between the various subspaces formed from the Q21A data. Each subspace is colored differently with the intensity of the color corresponding to detection statistic. Stars indicate location of events used to create the subspace.

The impact of the source-receiver distance on the subspace detection performance was not significant for the surface mine, but was significant for the underground coal mines. This difference probably occurs because most surface blasts were above the sensitive magnitude range; by design all blasts must exert some minimum amount of energy in order to be useful in mining efforts.

The subspace detectors were able to detect several events with moderate magnitudes (M_d > 1.25) that were not cataloged by the NF array, but were easily identifiable in the helicorder records. For the combined results of Q20A and Q21A, the number of verified event detections vs. detection threshold curve matched closely in shape to the number of possible false detections curve (Figure 4a, solid and dotted green lines). One interpretation of the similarity is that all, or nearly all, of the possible false detections occurring on both stations are real events from the mining district that were missed by the NF network. In this case, subspace detection provides a useful means of augmenting conventional seismic catalogs by both finding events that were missed above a detectable magnitude, and possibly finding events below the detectable magnitude that are very similar to training events. In addition, the events detected by a subspace that are located far from most other events detected by the same subspace (Figure 4c) are possibly misallocated. Such events could be flagged and subjected to extra scrutiny in order to improve the quality of locations in the catalog.

The spatial correlation between events detected by a given subspace provides a way to estimate the epicentral location, as well as to broadly classify the event into some pre-determined group, in this case to a particular pit or mine, with data from as little as one station. Event classification through subspace detection and waveform similarity is a powerful tool in discriminating one class of event from another (e.g. MIS from earthquakes or chemical blasts) because the classification is sensitive to both source and location (Equation 1).

Although we were not able to identify all of the events in the blasting log or NF catalog, the subspace methods applied in this study were able to greatly increase the detection capabilities of the regional TA stations. The same subspace methods might also be applied to local array data in order to increase catalog completeness. If sufficient stations are used in the detection process, double difference epicenter locations (Waldhauser and Ellsworth, 2000) could be calculated, which is a focus of future work.

ACKNOWLEDGEMENTS

Funding for this research was provided by the National Institute for Occupational Health and Safety (NIOSH). The support of NIOSH is thankfully acknowledged; however the conclusions expressed in this paper are those of the authors and do not represent the opinions or policies of NIOSH.

Additionally, the authors would like to thank OMSHR and Westmoreland Kemmerer Inc. for providing the data used to verify our work.

REFERENCES

Anstey, N.A. (1966). “Correlation Techniques—A Review”, Can. J. Expl. Geo-phys., 2, 55–82.

Array Network Facility. (2013). Archived Events. http://anf.ucsd.edu. Accessed November 2014.

Astiz, L., Eakins J.A., Martynov V.G., Cox, T.A., Tytell, J., Reyes, J.C., Newman, R.L., Gulsum, H.K, Mulder, T., White, M., Davis, G.A., Busby R.W., Hafner, K., Meyer J.C., and Vernon, F.L. (2014). "The Array Network Facility Seismic Bulletin: Products and an unbiased view of United States seismicity." Seismol. Res. Lett. 85:576–593

Bensen, G. D., Ritzwoller, M. H., Barmin, M. P., Levshin, A. L., Lin, F., Moschetti, M. P., Shapiro, N. M., and Yang, Y. (2007). "Processing seismic ambient noise data to obtain reliable broad-band surface wave dispersion measurements." Geophys. J. Int., 169, 1239- 1260.

Bonner, J.L., Pearson, D.C. and Blomberg, W.S. (2003). "Azimuthal Variation of Short-Period Rayleigh Waves from Cast Blasts in Northern Arizona." Bull. seism. Soc. Am., 93, 724– 736.

Dodge, D. A., and Walter, W. R. (2015). "Initial Global Seismic Cross-Correlation Results: Implications for Empirical Signal Detectors." Bulletin of the Seismological Society of America, February 2015, v. 105, p. 240-256.

Gibbons, S. J., & Ringdal, F. (2006). "The detection of low magnitude seismic events using array-based waveform correlation." Geophysical Journal International, 165(1), 149-166.

Harris, D. (2006). "Subspace detectors: Theory." Lawrence Livermore Natl. Lab. Rep. UCRL- TR-222758, Lawrence Livermore National Laboratory, Livermore, California. [https://e- reports-ext.llnl.gov/pdf/335299.pdf]

Houser, C., Masters., G., Shearer, P., and Laske, G. (2008). "Shear and compressional velocity models of the mantle from cluster analysis of long period waveforms." *Geophys. J. Int.* 174:195-212.

Johnson, C., Bittenbinder, A. Bogart, B., Dietz, L., and Kohler, W. (1996) "Earthworm : A flexible approach to seismic network processing." Iris newsletter. [http://www.iris.iris.edu/newsletter/FallNewsletter/earthworm.html].

Kubacki, T., Koper, K.D., Pankow, K.L., and McCarter, M.K. (2014). "Changes in mining-Induced seismicity before and after the 2007 Crandall Canyon Mine collapse." J. Geophys. Res. Solid Earth 119: 4876–4889.

Luxbacher, K., Westman, E., Swanson, P., and Karfakis, M. (2008). "Three-dimensional time-lapse velocity tomography of an underground longwall panel." International Journal of Rock Mechanics and Mining Sciences, 45 (4), pp. 478-485.

McLaughlin, K.L., Bonner, J.L. and Barker, T. (2004). "Seismic source mechanisms for quarry blasts: modelling observed Rayleigh and Love wave patterns from a Texas quarry." Geophys. J. Int., 156, 79–93.

Megies, T., Beyreuther, M., Barsch, R., Krischer, L., and Wassermann, J. (2011). "ObsPy – What can it do for data centers and observatories?" *Ann. Geophys.* 54(1):47–58. [http://www.annalsofgeophysics.eu/index.php/annals/article/view/4838]

Mendecki, A. J., Ed. (1997). "Seismic Monitoring in Mines." Chapman & Hall, London

Mercer, R.A., and Bawden, W.F. (2005). "A statistical approach for the integrated analysis of mine-induced seismicity and numerical stress estimates, a case study - Part I: Developing the relations." International Journal of Rock Mechanics and Mining Sciences, 42 (1), pp. 47-72.

Richards, P. G., Waldhauser, F., Schaff, D., and Kim, W. Y. (2006). "The applicability of modern methods of earthquake location." Pure and Applied Geophysics, 163(2-3), 351- 372.

Slinkard, M., Schaff, D., Mikhailova, N., Heck, S., Young, C., & Richards, P. G. (2014). "Multistation Validation of Waveform Correlation Techniques as Applied to Broad Regional Monitoring." Bulletin of the Seismological Society of America, 104(6), 2768- 2781.

Stein, S., and Wysession, M. (2009). "An introduction to seismology, earthquakes, and earth structure." John Wiley & Sons.

Stump, B.W., Hayward, C.T., Hetzer, C., and Zhou R.M. (2001). "Utilization of seismic and infrasound signals for characterizing mining explosions." Proc. 23rd Seismic Research Review on Worldwide Monitoring of Nuclear Explosions, 2-5 October 2001, Jackson, Wyoming.

Swanson, P., Steward, C., and Koontz, W. (2008). "Monitoring Coal Mine Seismicity with an Automated Wireless Digital Strong-Motion Network." 27th International Conference on Ground Control in Mining. [http://www.cdc.gov/niosh/mining/userfiles/works/pdfs/mcmsw.pdf]

Waldhauser, F., and Ellsworth, W.L. (2000). "A double-difference earthquake location algorithm: method and application to the northern Haywood fault." Bulletin of the Seismological Society of America. 90:1353–1368.

Proceedings
34th International Conference on Ground Control in Mining

Edited by

Thomas Barczak[5]
Syd S. Peng[8]
Donna Schmidt[4]
Steve Tadolini[6]
Melanie Thompson[3]

Primary Technical Reviewers

Donovan Benton[7]
Dennis Dolinar[11]
Essie Esterhuizen[7]
Keith Heasley[8]
Ted Klemetti[7]
Brijes Mishra[8]
Michael Murphy[7]
Dan Payne[2]
Kyle Perry[9]
Steve Tadolini[6]
Ihsan Tulu[7]
Erik Westman[10]
Peter Zhang[1]

1. Alpha Natural Resources
2. BHP Billiton Mitsubishi Alliance
3. Consultant (Freelance Editor)
4. Editorial consultant and Coal Age Field Editor
5 ICGCM Inc.
6 Orica
7. NIOSH, Office of Mine Safety and Health Research
8. West Virginia University
9. University of Kentucky
10 Virginia Tech
11. Retired (NIOSH)

July 28 - 30, 2015